




Microscope and micro-camera assessment of Schneiderian membrane perforation via transcrestal sinus floor elevation: A randomized ex vivo study

Jordi Gargallo-Albiol^{1,2}  | Khaled H. Sinjab¹ | Shayan Barootchi¹  |
Hsun-Liang Chan¹ | Hom-Lay Wang¹ 

¹Department of Periodontics and Oral Medicine, University of Michigan School of Dentistry, Ann Arbor, Michigan

²Oral and Maxillo-facial Surgery Department, Universitat Internacional de Catalunya, Barcelona, Spain

Correspondence

Jordi Gargallo-Albiol, Department of Periodontics and Oral Medicine, University of Michigan, Ann Arbor, MI.
Email: jgargallo@uic.es

Funding information

This paper was partially supported by the University of Michigan Periodontal Graduate Student Research Fund.

Abstract

Objective: We sought to assess the effectiveness of using a microscope and non-invasive camera for assessing sinus membrane perforations during transcrestal sinus floor elevation (TSFE).

Materials and methods: Five fresh human cadaver heads corresponding to eight maxillary sinuses (six bilateral and two unilateral) underwent 4 TSFEs per sinus (a total of 32 single site elevations). Each elevation was randomly assigned to receive a three or six mm membrane elevation height (MEH). A microscope and micro-camera were used to assess the sinus membrane perforation. Afterwards, radiological and clinical membrane perforation assessments were performed. The statistical analysis results are expressed using the means, standard deviations, range values of the residual ridge height (RRH), residual ridge width (RRW), sinus membrane thickness (SMT) and incidence of perforation (IoP). Generalized linear methods were used to test for the correlation of RRH and MEH to the microscope and micro-camera perforation assessments and the correlation of microscope and micro-camera assessments with the post-operative CBCT and crestal liquid evaluation.

Results: The cumulative percentage of IoP was 40.62%, (23.07% with 3 mm MEH, and 76.92% with 6 mm MEH, $p < 0.05$). The perforation assessed using either the microscope or micro-camera coincided with the post-operative CBCT and crestal liquid assessment in 87.55% sites. No significant correlation was found between the microscope or micro-camera assessments with RRH or MEH.

Conclusion: Application of a microscope and micro-camera during transcrestal sinus floor elevation may allow the detection of the integrity of the Schneiderian membrane with greater than 85% accuracy in this ex vivo model.

KEYWORDS

clinical assessment, diagnosis, sinus floor elevation

1 | INTRODUCTION

Maxillary sinus augmentation procedures are indicated to overcome vertical bone deficiencies in the posterior maxilla to allow longer implant placement (Boyne & James, 1980). Transcrestal sinus floor elevation (TSFE) was performed by lifting the sinus floor via sequential crestal bone preparations (Summers, 1994; Tatum, 1986). The TSFE approach is less invasive and less traumatic with high patient acceptance and reduced post-operative discomfort compared with the lateral window approach (Emmerich, Att, & Stappert, 2005). However, Schneiderian membrane perforations are common intra-operative complications (Garbacea et al., 2012; Yassin Alsabbagh, Alsabbagh, Darjazini Nahas, & Rajih, 2017). These perforations are generally undetectable by the operator during the surgical procedure, thus eventually leading to further post-surgical complications (Nolan, Freeman, & Kraut, 2014). Recently, other improved TSFE has been proposed; these include but are not limited to the balloon technique (Chan et al., 2013; Yassin Alsabbagh et al., 2017), the hydraulic elevation technique (Bensaha, 2011; Better et al., 2018; Tallarico, Better, De Riu, & Meloni, 2016), the piezotome technique and the reamer system (Yassin Alsabbagh et al., 2017). Among the TSFE techniques proposed, the reamer system (e.g., SCA-Neobiotech, Seoul, South Korea) exhibits less trauma compared with other TSFE techniques (Gargallo-Albiol, Tattan, Sinjab, Chan, & Wang, 2018; Kim, Lee, Park, Kim, & Oh, 2017; Yassin Alsabbagh et al., 2017).

The ability of detecting a sinus membrane perforation may influence treatment approach during TSFE, such as place implant with or without bone grafting, delay implant placement or even performed sinus lifting via the lateral approach. Nevertheless, the detection of a membrane perforation during and following TSFE is very challenging. Cone beam computed tomography (CBCT) and periapical digital radiography are not precise methods to detect these perforations (Garbacea et al., 2012). In an attempt to improve surgical outcomes and reduce complications, the operating microscope was introduced to dentistry (Bonsor, 2015; Khalighinejad et al., 2017; Setzer, Kohli, Shah, Karabucak, & Kim, 2012; Wang, Zhang, Wang, Jiang, & Liang, 2017). This microscope level of magnification ($\geq 6-8\times$) combined with a coaxial illumination enhances the operator's vision during surgery, thus reducing potential post-surgical complications (Bonsor, 2015; Mamoun, 2016). Additionally, telemedicine has been penetrating the surgical field in search of methods to overcome the limitations of conventional treatments through the use of high-definition images for better diagnosis of pathologies (Moberly et al., 2018).

Therefore, this study sought to investigate the effectiveness of using a microscope and non-invasive camera to assess sinus membrane perforations after TSFE and to analyse the influence of the membrane elevation height (MEH) and the residual ridge height (RRH) on the intra-operative microscope and camera assessment methods and the incidence of membrane perforations (IoP).

2 | MATERIALS AND METHODS

This project was in accordance with the EQUATOR guidelines Standards for Reporting Qualitative Research (SRQR) (O'Brien, Harris, Beckman, Reed, & Cook, 2014).

2.1 | Study design

Five fresh human cadaver heads with full or partially edentulous maxillary arches were provided by the Department of Anatomy at the University of Michigan. These specimens were frozen at a temperature of -20°C after being harvested from human donors to prevent structural changes in the tissues. Prior to being used in this study, the cadaver heads were completely thawed for a period of 4 to 5 days at room temperature. The University of Michigan (U-M) Institutional Review Board approved this study as exempt from oversight (HUM00149918).

The included cadaver heads corresponding to eight maxillary sinuses (six bilateral sinuses with fully edentulous arches and two unilateral sinuses with partially edentulous arch) underwent 4 TSFE procedures per sinus (a total of 32 elevations). Each elevation was randomly assigned to receive a different MEH using specialized software (randomized.com, Shogun Interactive Development 2006). The number 1 indicated 3 mm height elevation, and the number 2 indicated 6 mm height elevation. All membrane elevations were performed using the Sinus Crestal Approach (SCA) drill kit (Neobiotech).

2.2 | Eligibility criteria

The inclusion criteria included the following:

- Completely or partially edentulous posterior maxillary arches.
- Absence of sinus pathology evident in three-dimensional pre-surgical radiological assessment.
- No sinus septa existed as pre-surgically examined using CBCT.

Specimens were excluded based on the following:

- The posterior maxillary arch was fully dentated, preventing a transcrestal sinus elevation.
- A posterior maxillary arch width < 2 mm.
- Detection of a large sinus pathology via pre-procedural CBCT imaging.

2.3 | CBCT data acquisition

Tenting screws (Master-Pin-Control Fixation System, Osteogenics Biomedical, Inc.) were inserted mesial to each maxillary sinus near the maxillary canine area in fully edentulous arches. These screws functioned as reference points that were visible in the CBCT imaging for measurements and identification of precise drilling sites to be made

across the arch during the surgical procedure. In partially edentulous arches, the remaining teeth provided these references. The CBCT scans were obtained by a qualified operator (KS) in the Radiology Department at the University of Michigan, School of Dentistry. The specimens were stabilized using a head locator. Each maxillary sinus was pre-surgically examined in CBCT scans (3D Accuitomo 170 Tomograph, J Morita) with a voxel size of 0.08–0.16 mm. The operating parameters were set at 5.0–7.0 mA and 90 kV. Exposure time was 17.5 s. Limited FOV was selected for all images. CBCT scans of each head were reconstructed with the built-in software and analysed on a desktop computer with a specialized implant planning software (Invivo5, InvivoDent, Anatomage). CBCT images were evaluated by an experienced oral surgeon (JG). CBCT images were reoriented to reveal the following: (a) the nasal spine and midline aligned in the centre of the image in the axial slice; (b) the posterior maxillary segment in the vertical position in the coronal slices; and (c) the hard palate as well as the floor of the nose in a horizontal position parallel to the ground in the sagittal slices. For the evaluation of intra-examiner reliability, all measurements were performed twice, and each measurement was performed on a different day. The mean difference between the two measurements in bone parameters was 0.01 mm (range –0.059–0.079). For image assessment, each sample was assessed twice, and a mean value was obtained (Janner et al., 2011). If $a \geq 0.2$ mm difference was measured at the same point, a third assessment was performed (Bornstein, Lauber, Sendi, & von Arx, 2011; Froum, Khouly, Favero, & Cho, 2013). Similarly, a second examiner (SB) randomly selected two cases to evaluate inter-examiner reliability, where a 0.86 interclass correlation coefficient was obtained, indicating good agreement.

2.4 | Surgical procedure

An experienced surgeon (JG) performed the surgical procedures according to the CBCT pre-surgical analysis and measurements. A mid-crestal incision and a mesial vertical releasing incision above the canine area were performed to elevate a full thickness flap. CBCT measurements made from the tenting screws to the planned drill sites were extrapolated to the surgical set-up, where the same measurements were made using the exposed bone (Figure 1). Bone preparation was performed following the SCA drill kit manufacturer's guidelines. The preparation depth was determined based on the RRH that was pre-surgically measured on the CBCT images.

2.5 | Sinus membrane elevation

The osteotomies were initiated using a 2-mm round drill to mark the sites according to the CBCT planning and the reference points. Afterwards, SCA drills increasing from 2.4 to 3.2 in diameter and connected with a stopper were used to complete the bone preparation (Figure 2). Stoppers defined the drilling length according to RRH and MEH. The MEH was randomly determined between 3 or 6 mm and was measured using a calibrated gauge.

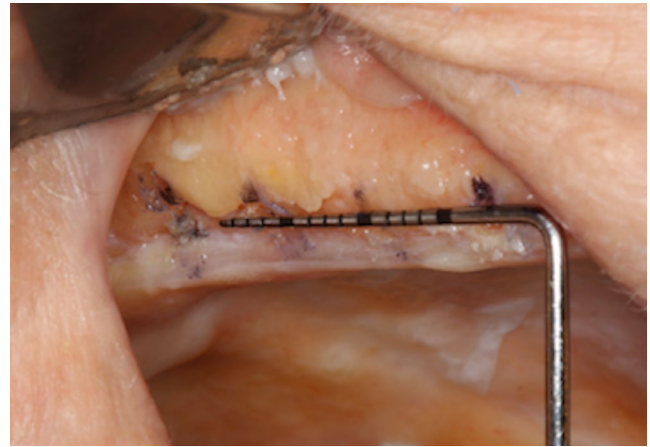


FIGURE 1 Bone marking measurements of the planned drill sites

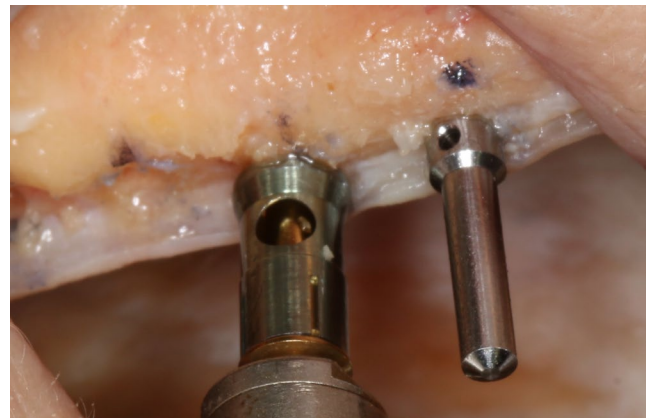


FIGURE 2 Bone preparations using the sinus crest approach (SCA) drill kit

2.6 | Data retrieval

RRH, width and sinus membrane thickness (SMT) were pre-surgically evaluated at each elevation site in relation to the reference point (tenting screw or retained tooth) viewed in the pre-surgical CBCT scans. After sinus membrane elevation, two devices were used by two different investigators (KS and SB) to clinically assess the sinus membrane perforation: (a) a microscope (Suzhou Semorr Medical Tech Co., Ltd.) with an objective lens of $f = 250$ mm (0–16 mm focusable) and eyepieces (18 mm of aperture and 12.5× to 18× augmentation) with inclinable binoculars (0–210 degrees), including a LED illumination source (85 mm of diameter of illumination spot); and (b) a micro-camera (USB Oscope Camera, Depstech) with 6 LED adjustable lights, 0.3 megapixels, 640–480 resolution, and a focal length of 20–30 mm compatible with android, windows and mac devices using a micro USB adaptor.

Intra-surgical images were obtained and viewed on a 22-inch Full High Definition SuperClear® in-plane switching (IPS) LED multimedia display (Viewsonic) when using the microscope and on a

MacBook air, 11.6-inch laptop computer with high-definition LED LCD screen when using the micro-camera.

After the microscope and micro-camera evaluation was completed, a bony window on the lateral wall of the maxillary sinus was performed apical to the crestal bone preparations using the Sinus Lateral Approach kit (Neobiotech). At that point, the sinus membrane was exposed and assessed for complete defrosting. Then, radiological and clinical membrane perforation assessment methods were performed as follows: (a) a post-operative CBCT with radiopaque contrast; (b) liquid communication from the crestal preparation to the maxillary sinus cavity.

For the CBCT assessment, polyvinyl siloxane light body impression material (Kerr Dental) was placed to seal every bony perforation from the crestal side. Then, once the specimens were stabilized with the head locator and prior to performing the CBCT scans, a radiopaque liquid made from mixing water and barium sulphate was introduced in each maxillary sinus cavity through the lateral window performed using a 23-gauge needle and a 5-cc syringe. The radiopacity of this liquid was previously checked with x-ray assessment. A post-operative CBCT was performed using the same standardized parameters described (3D Accuitomo 170 Tomograph, J Morita).

Afterwards, the specimens were again translated to the operating room to perform the liquid communication assessment. For this assessment, polyvinyl siloxane stoppers were removed with an exploration probe. Then, the same radiopaque liquid was introduced by one operator (JG) from the crestal site of each bone preparation using a 23-gauge needle and a 5-cc syringe. Two observers (KS and SB) assessed the communication of the liquid from the crestal bone preparation into the maxillary sinus cavity for each bone preparation site.

3 | MEASUREMENTS

The elevations were measured (in millimetres) from the alveolar crest to the topmost point. The MEH was calculated as the final membrane height minus the RRH.

CBCT images before and after the surgery were obtained, and intra-operative microscope and micro-camera evaluation as well as crestal liquid communication assessment were achieved. All the following measurements were obtained and recorded for each of the four elevation sites per maxillary sinus:

- Residual ridge height (RRH) (mm).
- Residual ridge width (RRW) (mm).
- Sinus membrane thickness (SMT) (mm).
- Membrane elevation height (MEH) (mm).
- Incidence of perforation according to microscope evaluation (micro-loP) (1–0).
- Incidence of perforation according to camera evaluation (cam-loP) (1–0).
- Incidence of perforation according to post-operative CBCT (CBCT-loP) (1–0).
- Incidence of perforation according to post-operative crestal liquid evaluation (liquid-loP) (1–0).

3.1 | Statistical analysis

Means and standard deviations (SD) were calculated for continuous outcomes of RRH, RRW, SMT and loP. The Fisher's exact test was used for comparing the perforation rates between the 3 and 6 mm elevation groups, and linear mixed-effects regression models were produced (for control for repeated measures, such as each cadaver head that contributed to multiple sinus elevation procedures with random intercepts) to test for the correlation of loP with RRH, RRW, SMT and MEH; the correlation of RRH and MEH with microscope and micro-camera assessment; and finally the correlation of the intra-operative microscope and micro-camera assessment with the post-operative CBCT and crestal liquid evaluation. Confidence intervals (CI) were produced, and a *p*-value threshold of 0.05 was set for statistical significance. All analyses were conducted by an author with expertise in statistical analyses using Rstudio (Rstudio Version 1.1.383, Rstudio, Inc.) lme4 (Bates, Mächler, Bolker, & Walker, 2015) package.

4 | RESULTS

4.1 | Descriptive analysis

We excluded two unilateral sinuses given the dentate ridges that made it difficult to standardized as all other included sinuses were either a full or partially edentulous ridges. Furthermore, we also excluded 8 of 32 elevation sites because image artefacts/distortion was noted in the pre-operative CBCT, which made it impossible to accurately measure the region of interest. Based on the remaining 26 sites, the mean membrane thickness was 0.64 ± 0.20 mm. The mean ridge height and mean ridge width were 5.03 ± 2.28 and 8.62 ± 3.69 mm, respectively. A complete descriptive analysis of the data is presented in Table 1.

4.2 | Incidence of Schneiderian membrane perforation

The cumulative percentage of loP for all the assessed samples with the post-operative CBCT images or the post-operative crestal liquid was 40.62%, that is, 23.07% in group 1 (3 mm of MEH) and 76.92% in group 2 (6 mm of MEH), coinciding the two evaluation methods. The difference between the two groups was statistically significant with an odds ratio of 9.88 (95% CI [1.38, 101.51], *p* = 0.01). The significant difference in perforation rate between the two groups of elevation height reveals that perforation is dependent on the MEH with increased loP when a 6 mm MEH is indicated compared with 3 mm MEH.

On the other hand, no statistically significant correlation was found between the loP and the RRH (*p* = 0.85) with an estimated coefficient of -0.159 (95% CI $[-1.86, 1.54]$). No statistical significances were also observed between the loP and RRW (*p* = 0.67) with an estimated coefficient of -0.56 (95% CI $[-3.32, 2.18]$) and between loP and SMT (*p* = 0.52) with an estimated coefficient of 0.05 (95% CI $[-0.12, 0.24]$).

TABLE 1 Descriptive analysis of the data

N	Random	Residual ridge height (mm)	Residual ridge width (mm)	Membrane thickness (mm)	Microscope PERFO (Y/N)	Camera PERFO (Y/N)	CBCT post PERFO (Y/N)	Clinical liquid PERFO (Y/N)
1	1	8.42	7.61	0.7	Y	Y	Y	Y
2	2	3.58	13.02	0.62	Y	Y	Y	Y
3	2	3.13	11.81	1.2	N	N	Y	Y
4	2	4.18	17.75	0.6	N	N	N	N
5	2	7.01	9.45	0.79	Y	Y	Y	Y
6	2	4.04	14.4	0.53	Y	Y	N	N
7	2	2.87	14.78	0.53	Y	Y	Y	Y
8	1	3.99	14.61	0.69	Y	Y	N	N
9	1	10.0	4.35	NA	N	N	N	N
10	1	9.5	5.85	NA	N	N	N	N
11	2	7.87	6.56	NA	N	Y	N	Y
12	2	6.16	5.06	NA	Y	Y	Y	Y
13	2	3.93	7.52	0.5	Y	Y	Y	Y
14	2	7.44	7.85	0.83	Y	Y	N	N
15	2	5.38	6.63	0.5	N	N	N	N
16	1	2.70	9.70	0.6	Y	Y	N	Y
17	2	6.21	5.94	0.3	N	N	Y	N
18	1	6.33	7.68	0.4	N	N	N	N
19	1	6.61	8.95	0.57	N	N	N	N
20	1	4.20	9.57	0.72	N	N	N	N
21	1	7.18	2.94	NA	N	N	N	N
22	2	5.35	3.01	NA	Y	Y	Y	Y
23	2	2.96	3.00	NA	Y	Y	Y	Y
24	1	4.22	11.39	NA	Y	Y	Y	Y
25	2	6.42	8.60	0.68	N	N	N	N
26	2	2.70	9.99	0.46	N	N	N	N
27	1	3.04	10.06	1.01	N	N	Y	N
28	1	5.18	11.45	0.93	N	N	N	N
29	2	5.97	4.84	0.49	Y	Y	Y	Y
30	2	1.02	4.93	0.57	N	N	N	N
31	1	2.03	8.53	0.72	N	N	N	N
32	1	1.37	8.18	0.42	N	N	N	N

Note: Random MEH: 1 (3 mm), 2 (6 mm); Y: yes; N: no; Green boxes indicate when all correlation assessment techniques were consistent.

4.3 | Correlation of intra-operative and post-operative assessment methods

The perforations assessed using either intra-operative microscope (Figure 3) or micro-camera (Figure 4) coincided with the post-operative CBCT (Figure 5) and post-operative crestal liquid assessment in 87.55% sites (28/32 sites). Otherwise, in 75% sites (24 of 32 sites), full agreement of the four methods (intra-operative microscope and micro-camera, and post-operative CBCT and crestal liquid) was noted. Detailed description of the IoP relating to the assessment methods and their correlation is described in Table 2.

4.4 | RRH and MEH influence on intra-operative assessment methods

No significant correlation was found between the microscope assessment and RRH (estimated coefficient of -0.22 (95% CI $[-1.91, 1.46]$), $p = 0.78$) or between the use of the micro-camera and the RRH (estimated coefficient 0.13 (95% CI $[-1.54, 1.81]$), $p = 0.87$). In addition, no significant correlation was found when using the microscope assessment in relation to the MEH (3 or 6 mm) (estimated coefficient 0.26 (95% CI $[-0.08, 0.62]$), $p = 0.13$) and between the use of the micro-camera assessment and the MEH (estimated coefficient 0.32 (95% CI $[-0.02, 0.67]$), $p = 0.71$). The

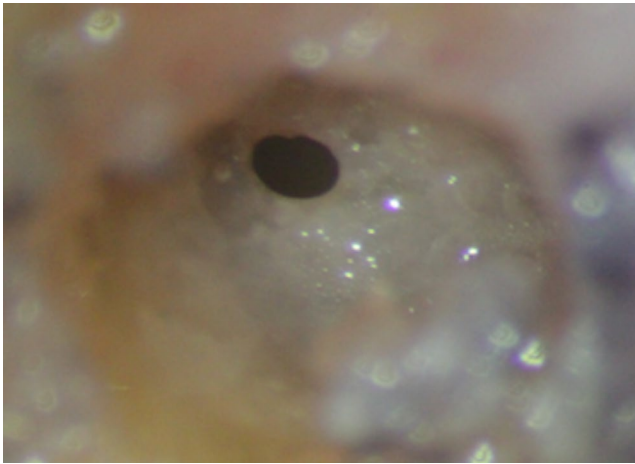


FIGURE 3 Intra-surgical image of a sinus membrane perforation using the microscope

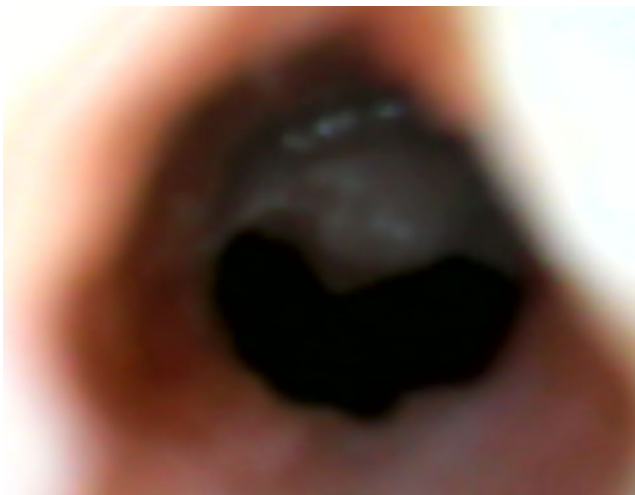


FIGURE 4 Intra-surgical image of a sinus membrane perforation using the micro-camera

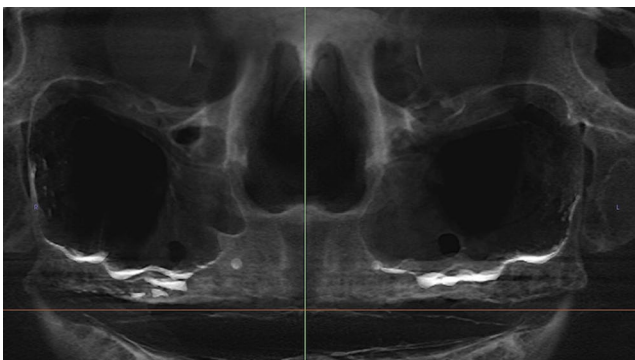


FIGURE 5 Post-operative CBCT assessment with a radiopaque contrast

lack of a significant correlation shows that the efficacy of the operating microscope and the micro-camera in detecting sinus membrane perforation during TSFE is independent of the RRH or sinus MEH.

5 | DISCUSSION

Increased patient morbidity during TSFE, such as that manifested by pain and analgesic consumption, has not been studied in detail (Franceschetti et al., 2017; Soardi et al., 2013; Trombelli et al., 2010). Sinus membrane perforations are the most common type of complication in TSFE surgeries (Andreasi Bassi et al., 2016; Wen, Lin, Yang, & Wang, 2015). Without membrane perforation, post-operative complications following TSFE procedures should be minimal to none (Danesh-Sani, Loomer, & Wallace, 2016; Franceschetti et al., 2017; Moreno Vazquez, Gonzalez de Rivera, Gil, & Mifsut, 2014). A small Schneiderian membrane perforation during TSFE may push the bone graft material into the sinus cavity, leading to mucosal thickening, maxillary sinusitis, infection and other complications (Chen et al., 2018). According to Chirila et al., 4.3% patients developed maxillary sinusitis after TSFE procedures related to sinus membrane perforations (Chirila, Rotaru, Filipov, & Sandulescu, 2016). The perforations have also been associated with secondary infections, chronic sinusitis, an increase consumption of antibiotic, loss of bone graft and implant failure (Alkan, Celebi, & Bas, 2008; Beltramini, Lagana, Gianni, & Baj, 2013; Katranji, Fotek, & Wang, 2008; Matern et al., 2016; Nolan et al., 2014). Hence, it is important to detect the perforation during surgery to avoid all these potential complications before they occur. In this study, the mean IoP rate of 40.62% was similar to the data reported by Cho, Wallace, Froum, and Tarnow (2001), Garbacea et al. (2012) or Nolan et al. (2014), who reported mean IoP rates of 37.5%, 40% and 41%, respectively. These rates were considerably less than the 58.4% reported by Alsabbagh AY (Yassin Alsabbagh et al., 2017) using the osteotome technique. However, the rate was considerably increased compared with the 17.30% perforation rate reported by Wen et al. (2015) in a clinical retrospective setting using the direct visualization or the Valsalva manoeuvre to detect membrane perforations complemented with the immediate post-operative CBCT exploration, which might be less accurate than the ex vivo evaluation.

In the event of a membrane perforation during TSFE surgery, management of the perforation is recommended at the time of surgery. Andreasi Bassi et al. (2016) created a bony tunnel through the buccal mucosa apical to the TSFE to place the endoscope to cover the perforated area with an absorbable collagen membrane. Endoscopic sinus surgery can also be used to correct post-operative infection (e.g., chronic rhinosinusitis) associated with TSFE procedures (Jiam, Goldberg, Murr, & Pletcher, 2017). If these infections were not properly managed, it may lead to more severe complications and life-threatening conditions, such a brain abscess (Manor & Garfunkel, 2018). Hence, despite the report of the low incidence of complications during or after TSFE surgeries, clinicians must focus on early detection of membrane perforation during surgery to avoid unnecessary consequences (Kim et al., 2017).

The industrial expansion of telemedicine has resulted in the development of many new tools/devices to overcome surgical limitations and achieve better clinical outcomes (Moberly et al., 2018). However, this technological revolution must be supported by sound evidence. In this study, the use of a low-cost otoscope camera has

TABLE 2 Incidence of the Schneiderian membrane perforation and the correlation of assessment methods

	n	%
Elevations	32	100
Clinical and CBCT assessment perforations	13	40.62
Clinical and CBCT assessment perforations in group 1 VEH (3 mm)	3	23.07
Clinical and CBCT assessment perforations in group 2 VEH (6 mm)	10	76.92
Clinical and CBCT assessment no perforations	19	59.37
Correlation camera-clinic assessment	28	87.5
Correlation microscope-clinic assessment	28	87.5
Correlation CBCT-clinic assessment	28	87.5
Correlation microscope-camera-CBCT-clinic assessment	24	75

demonstrated similar results as those noted in the operating microscope, allowing the intra-operative detection of 87.5% of sinus membrane perforations during TSFE surgery. The main difference between the two systems aside from the cost was the better quality of the images obtained when using the microscope. This information allows the clinician to decide whether to insert a bone graft during the TSFE. The TSFE technique without the insertion of bone graft biomaterials has shown a high success rate with minimal patient morbidity (Andreasi Bassi et al., 2016; Kaneko, Masuda, Horie, & Shimoyama, 2012). Hence, it is important to note that once a sinus membrane perforation is detected during TSFE surgery, avoiding bone graft insertion might prevent the incidence of post-operative maxillary sinus complications.

SMT (Wen et al., 2015), the presence of sinus septa (Al-Dajani, 2016), RRH (Schwarz et al., 2015) and MEH (Lundgren et al., 2017) have all been described as factors related to IoP during TSFE procedures. The mean SMT was 0.64 ± 0.2 mm in our study, which correlates to the findings of Wen et al. (2015) and Insua, Monje, Urban, et al. (2017)). However, the CBCT assessment was 2.6-fold higher than the histological examination (Insua, Monje, Chan, et al., 2017). In our study, no correlation was found between the membrane thickness and the IoP, which is contrary to the findings reported by Wen and co-workers (Wen et al., 2015) who observed a higher perforation rate in thicker membranes (≥ 3 mm) or thinner membranes (< 0.5 mm). These findings are partially in contrast to the findings of Al-Dajani (2016) who found reduced thickness to be a factor predisposing sinus membrane perforation. The lack of correlation of the SMT with the IoP in this study could be explained by the smaller variation in thickness in our sample (0.64 ± 0.20 mm) due to our strict exclusion criteria involving pre-operative CBCT sinus pathology and the limited sample size.

Additionally, the variations among the RRH observed in our study (mean 5.03 ± 2.28) do not seem to have an influence on the IoP despite the findings of Schwarz et al. (2015) and Lundgren et al. (2017), who recommended a minimal RRH of 3.5 mm and 5 mm, respectively, to reduce the IoP during TSFE. The difference probably could be explained by the fact that this study only used the SCA

reamer system with an experienced surgeon and the lack of bone graft insertion or implant placement, which limit the chance of membrane perforations as noted in the above two studies.

A significant difference in perforation rate was found between the 3 and 6 mm elevation height groups in our study. These results indicate that the higher the membrane elevation, the higher the IoP. The finding is consistent with the observations by Lundgren et al. (2017), who reported that the elevation height in TSFE should not exceed 3–4 mm and also recommended a minimum RRH of 3.5 to 5 mm for the TSFE procedure (Lundgren et al., 2017; Schwarz et al., 2015). It is also important to note that several alternative approaches should also be considered during treatment planning, especially in the areas of RRH. These alternate options include but are not limited to short implants (4–6 mm of length) without TSFE or with limited SFE (Bechara et al., 2017; Gastaldi et al., 2017; Thoma, Cha, & Jung, 2017).

Several limitations should be acknowledged regarding the present study. For example, cadaver specimens were used, and their bone quality and membrane elasticity may differ from the living bone. To minimize the bias of specimen quality, we chose frozen fresh cadaver heads that most resemble tissue conditions of living patients. Nevertheless, this remains a concern of the present study. Additionally, the absence of bleeding provides less interference with the use of the imaging devices. This bias has to be minimized in real patients using constant aspiration before applying the imaging devices, assuming possible interference with the imaging results. Furthermore, intra-operative handling of the micro-camera and the microscope is quite complex and may require a learning curve. Finally, due to the nature of this research (limited access to cadaveric specimen), the sample size is a limitation that should be noted in the study. We only used available fresh cadaver heads that qualified for conducting this investigation, excluding those with pre-surgically detected maxillary sinus pathologies (through CBCT analysis) or teeth in the posterior maxilla.

In addition, an intra-operative control should be specified in clinical cases with micro-camera and microscope findings that are quite complex.

Finally, the application of new devices during surgical treatment represents an exciting panorama to overcome some treatment challenges. Future studies will be required to evaluate the ability and confidence of the images collected.

6 | CONCLUSIONS

Intra-operative application of the operating microscope and the micro-camera during transcrestal sinus floor elevation may detect Schneiderian membrane integrity with greater than 85% accuracy in this ex vivo model. Variations in the residual ridge height and sinus membrane elevation height do not affect the microscope and micro-camera assessment. Contrary, the incidence of perforation was dependent on membrane elevation height. Clinical detection of sinus membrane perforations with these imaging devices would allow adequate management of this complication, avoiding the accidental leakage of the bone graft into the maxillary sinus cavity and

potentially preventing post-operative complications, such as infections, sinusitis and dental implant failures.

ACKNOWLEDGEMENTS

The authors would like to express their sincere appreciation to Mr. Dean Mueller, Anatomical Donor Program Coordinator at the School of Medicine for providing the specimens and their gratitude to Alberto Monje (Department of Oral Surgery and Stomatology, University of Bern, Bern, Switzerland) for his assistance during the elaboration of this manuscript.

CONFLICT OF INTEREST

The authors do not have any financial interests, directly or indirectly, in the products or information listed in the paper.

AUTHOR CONTRIBUTION

J.G conceived the idea and performed the research and writing. K.S performed the research and reviewed the manuscript. SB performed the research, analysed the data and reviewed the manuscript. HC performed the research and reviewed the manuscript. HLW conceived the idea and reviewed the manuscript.

ORCID

Jordi Gargallo-Albiol  <https://orcid.org/0000-0002-9307-8258>

Shayan Barootchi  <https://orcid.org/0000-0002-5347-6577>

Hom-Lay Wang  <https://orcid.org/0000-0003-4238-1799>

REFERENCES

- Al-Dajani, M. (2016). Incidence, Risk Factors, and Complications of Schneiderian Membrane Perforation in Sinus Lift Surgery: A Meta-Analysis. *Implant Dent*, 25(3), 409–415. <https://doi.org/10.1097/ID.0000000000000411>
- Alkan, A., Celebi, N., & Bas, B. (2008). Acute maxillary sinusitis associated with internal sinus lifting: Report of a case. *Eur J Dent*, 2(1), 69–72.
- Andreasi Bassi, M., Andrisani, C., Lico, S., Ormanier, Z., Barlattani, A. Jr, & Ottria, L. (2016). Endoscopic management of the schneiderian membrane perforation during transcrestal sinus augmentation: A case report. *Oral Implantol (Rome)*, 9(4), 157–163. <https://doi.org/10.11138/orl/2016.9.4.157>
- Bates, D., Mächler, M., Bolker, B., & Walker, S. (2015). Fitting Linear Mixed-Effects Models Using lme4. *Journal of Statistical Software*, 67(1), 48. <https://doi.org/10.18637/jss.v067.i01>.
- Bechara, S., Kubilius, R., Veronesi, G., Pires, J. T., Shibli, J. A., & Mangano, F. G. (2017). Short (6-mm) dental implants versus sinus floor elevation and placement of longer (>=10-mm) dental implants: A randomized controlled trial with a 3-year follow-up. *Clin Oral Implants Res*, 28(9), 1097–1107. <https://doi.org/10.1111/clr.12923>
- Beltramini, G. A., Lagana, F. C., Gianni, A. B., & Baj, A. (2013). Maxillary sinusitis after sinus lift due to Gemella morbillorum: Antibiotic and surgical treatment. *J Craniofac Surg*, 24(3), e275–276. <https://doi.org/10.1097/SCS.0b013e31828f2910>
- Bensaha, T. (2011). Evaluation of the capability of a new water lift system to reduce the risk of Schneiderian membrane perforation during sinus elevation. *International Journal of Oral and Maxillofacial Surgery*, 40(8), 815–820. <https://doi.org/10.1016/j.ijom.2011.04.005>
- Better, H., Chaushu, L., Nissan, J., Xavier, S., Tallarico, M., & Chaushu, G. (2018). The Feasibility of Flapless Approach to Sinus Augmentation Using an Implant Device Designed According to Residual Alveolar Ridge Height. *Int J Periodontics Restorative Dent*, 38(4), 601–606. <https://doi.org/10.11607/prd.2950>
- Bonsor, S. J. (2015). The use of the operating microscope in general dental practice. Part 2: If you can see it, you can treat it!. *Dent Update*, 42(1), 60–66. <https://doi.org/10.12968/denu.2015.42.1.60>
- Bornstein, M. M., Lauber, R., Sendi, P., & von Arx, T. (2011). Comparison of periapical radiography and limited cone-beam computed tomography in mandibular molars for analysis of anatomical landmarks before apical surgery. *J Endod*, 37(2), 151–157. <https://doi.org/10.1016/j.joen.2010.11.014>
- Boyne, P. J., & James, R. A. (1980). Grafting of the maxillary sinus floor with autogenous marrow and bone. *J Oral Surg*, 38(8), 613–616.
- Chan, H. L., Oh, T. J., Fu, J. H., Benavides, E., Avila-Ortiz, G., & Wang, H. L. (2013). Sinus augmentation via transcrestal approach: A comparison between the balloon and osteotome technique in a cadaver study. *Clin Oral Implants Res*, 24(9), 985–990. <https://doi.org/10.1111/j.1600-0501.2012.02506.x>
- Chen, Y. W., Lee, F. Y., Chang, P. H., Huang, C. C., Fu, C. H., Huang, C. C., & Lee, T. J. (2018). A paradigm for evaluation and management of the maxillary sinus before dental implantation. *Laryngoscope*, 128(6), 1261–1267. <https://doi.org/10.1002/lary.26856>
- Chirila, L., Rotaru, C., Filipov, I., & Sandulescu, M. (2016). Management of acute maxillary sinusitis after sinus bone grafting procedures with simultaneous dental implants placement - a retrospective study. *BMC Infectious Diseases*, 16(Suppl 1), 94. <https://doi.org/10.1186/s12879-016-1398-1>
- Cho, S. C., Wallace, S. S., Froum, S. J., & Tarnow, D. P. (2001). Influence of anatomy on Schneiderian membrane perforations during sinus elevation surgery: Three-dimensional analysis. *Practical Procedures & Aesthetic Dentistry*, 13(2), 160–163.
- Danesh-Sani, S. A., Loomer, P. M., & Wallace, S. S. (2016). A comprehensive clinical review of maxillary sinus floor elevation: Anatomy, techniques, biomaterials and complications. *British Journal of Oral and Maxillofacial Surgery*, 54(7), 724–730. <https://doi.org/10.1016/j.bjoms.2016.05.008>
- Emmerich, D., Att, W., & Stappert, C. (2005). Sinus floor elevation using osteotomes: A systematic review and meta-analysis. *Journal of Periodontology*, 76(8), 1237–1251. <https://doi.org/10.1902/jop.2005.76.8.1237>
- Franceschetti, G., Rizzi, A., Minenna, L., Pramstraller, M., Trombelli, L., & Farina, R. (2017). Patient-reported outcomes of implant placement performed concomitantly with transcrestal sinus floor elevation or entirely in native bone. *Clin Oral Implants Res*, 28(2), 156–162. <https://doi.org/10.1111/clr.12774>
- Froum, S. J., Khoully, I., Favero, G., & Cho, S. C. (2013). Effect of maxillary sinus membrane perforation on vital bone formation and implant survival: A retrospective study. *Journal of Periodontology*, 84(8), 1094–1099. <https://doi.org/10.1902/jop.2012.120458>
- Garbacea, A., Lozada, J. L., Church, C. A., Al-Ardah, A. J., Seiberling, K. A., Naylor, W. P., & Chen, J. W. (2012). The incidence of maxillary sinus membrane perforation during endoscopically assessed crestal sinus floor elevation: A pilot study. *J Oral Implantol*, 38(4), 345–359. <https://doi.org/10.1563/AID-JOI-D-12-00083>
- Gargallo-Albiol, J., Tattan, M., Sinjab, K. H., Chan, H. L., & Wang, H. L. (2018). Schneiderian Membrane Perforation via Transcrestal Sinus Floor Elevation: A Randomized Ex Vivo Study with Endoscopic Validation. *Clin Oral Implants Res*, 30(1), 11–19. <https://doi.org/10.1111/clr.13388>
- Gastaldi, G., Felice, P., Pistilli, R., Barausse, C., Trullenque-Eriksson, A., & Esposito, M. (2017). Short implants as an alternative to crestal

- sinus lift: A 3-year multicentre randomised controlled trial. *Eur J Oral Implantol*, 10(4), 391–400.
- Insua, A., Monje, A., Chan, H. L., Zimmo, N., Shaikh, L., & Wang, H. L. (2017). Accuracy of Schneiderian membrane thickness: A cone-beam computed tomography analysis with histological validation. *Clin Oral Implants Res*, 28(6), 654–661. <https://doi.org/10.1111/clr.12856>
- Insua, A., Monje, A., Urban, I., Kruger, L. G., Garaicoa-Pazmino, C., Sugai, J. V., & Wang, H. L. (2017). The Sinus Membrane-Maxillary Lateral Wall Complex: Histologic Description and Clinical Implications for Maxillary Sinus Floor Elevation. *Int J Periodontics Restorative Dent*, 37(6), e328–e336. <https://doi.org/10.11607/prd.3215>
- Janner, S. F., Caversaccio, M. D., Dubach, P., Sendi, P., Buser, D., & Bornstein, M. M. (2011). Characteristics and dimensions of the Schneiderian membrane: A radiographic analysis using cone beam computed tomography in patients referred for dental implant surgery in the posterior maxilla. *Clin Oral Implants Res*, 22(12), 1446–1453. <https://doi.org/10.1111/j.1600-0501.2010.02140.x>
- Jiam, N. T., Goldberg, A. N., Murr, A. H., & Pletcher, S. D. (2017). Surgical treatment of chronic rhinosinusitis after sinus lift. *Am J Rhinol Allergy*, 31(4), 271–275. <https://doi.org/10.2500/ajra.2017.31.4451>
- Kaneko, T., Masuda, I., Horie, N., & Shimoyama, T. (2012). New bone formation in nongrafted sinus lifting with space-maintaining management: A novel technique using a titanium bone fixation device. *Journal of Oral and Maxillofacial Surgery*, 70(3), e217–224. <https://doi.org/10.1016/j.joms.2011.10.025>
- Katranji, A., Fotek, P., & Wang, H. L. (2008). Sinus augmentation complications: Etiology and treatment. *Implant Dent*, 17(3), 339–349. <https://doi.org/10.1097/ID.0b013e3181815660>
- Khalighinejad, N., Aminoshariae, A., Kulild, J. C., Williams, K. A., Wang, J., & Mickel, A. (2017). The Effect of the Dental Operating Microscope on the Outcome of Nonsurgical Root Canal Treatment: A Retrospective Case-control Study. *Journal of Endodontics*, 43(5), 728–732. <https://doi.org/10.1016/j.joen.2017.01.015>
- Kim, Y. K., Lee, J. Y., Park, J. W., Kim, S. G., & Oh, J. S. (2017). Sinus Membrane Elevation by the Crestal Approach Using a Novel Drilling System. *Implant Dentistry*, 26(3), 351–356. <https://doi.org/10.1097/ID.0000000000000570>
- Lundgren, S., Cricchio, G., Hallman, M., Jungner, M., Rasmusson, L., & Sennerby, L. (2017). Sinus floor elevation procedures to enable implant placement and integration: techniques, biological aspects and clinical outcomes. *Periodontology 2000*, 73(1), 103–120. <https://doi.org/10.1111/prd.12165>
- Mamoun, J. S. (2016). The maxillary molar endodontic access opening: A microscope-based approach. *European Journal of Dentistry*, 10(3), 439–446. <https://doi.org/10.4103/1305-7456.184153>
- Manor, Y., & Garfunkel, A. A. (2018). Brain abscess following dental implant placement via crestal sinus lift - a case report. *European Journal of Oral Implantology*, 11(1), 113–117.
- Matern, J. F., Keller, P., Carvalho, J., Dillenseger, J. P., Veillon, F., & Bridonneau, T. (2016). Radiological sinus lift: A new minimally invasive CT-guided procedure for maxillary sinus floor elevation in implant dentistry. *Clinical Oral Implants Research*, 27(3), 341–347. <https://doi.org/10.1111/clr.12549>
- Moberly, A. C., Zhang, M., Yu, L., Gurcan, M., Senaras, C., Teknos, T. N., ... Essig, G. F. (2018). Digital otoscopy versus microscopy: How correct and confident are ear experts in their diagnoses? *Journal of Telemedicine and Telecare*, 24(7), 453–459. <https://doi.org/10.1177/1357633X17708531>
- Moreno Vazquez, J. C., Gonzalez de Rivera, A. S., Gil, H. S., & Mifsut, R. S. (2014). Complication rate in 200 consecutive sinus lift procedures: Guidelines for prevention and treatment. *Journal of Oral and Maxillofacial Surgery*, 72(5), 892–901. <https://doi.org/10.1016/j.joms.2013.11.023>
- Nolan, P. J., Freeman, K., & Kraut, R. A. (2014). Correlation between Schneiderian membrane perforation and sinus lift graft outcome: A retrospective evaluation of 359 augmented sinus. *Journal of Oral and Maxillofacial Surgery*, 72(1), 47–52. <https://doi.org/10.1016/j.joms.2013.07.020>
- O'Brien, B. C., Harris, I. B., Beckman, T. J., Reed, D. A., & Cook, D. A. (2014). Standards for reporting qualitative research: A synthesis of recommendations. *Academic Medicine*, 89(9), 1245–1251. <https://doi.org/10.1097/ACM.0000000000000388>
- Schwarz, L., Schiebel, V., Hof, M., Ulm, C., Watzek, G., & Pommer, B. (2015). Risk Factors of Membrane Perforation and Postoperative Complications in Sinus Floor Elevation Surgery: Review of 407 Augmentation Procedures. *Journal of Oral and Maxillofacial Surgery*, 73(7), 1275–1282. <https://doi.org/10.1016/j.joms.2015.01.039>
- Setzer, F. C., Kohli, M. R., Shah, S. B., Karabucak, B., & Kim, S. (2012). Outcome of endodontic surgery: A meta-analysis of the literature—Part 2: Comparison of endodontic microsurgical techniques with and without the use of higher magnification. *J Endod*, 38(1), 1–10. <https://doi.org/10.1016/j.joen.2011.09.021>
- Soardi, E., Cosci, F., Checchi, V., Pellegrino, G., Bozzoli, P., & Felice, P. (2013). Radiographic analysis of a transalveolar sinus-lift technique: A multipractice retrospective study with a mean follow-up of 5 years. *Journal of Periodontology*, 84(8), 1039–1047. <https://doi.org/10.1902/jop.2011.100684>
- Summers, R. B. (1994). A new concept in maxillary implant surgery: the osteotome technique. *Compendium*, 15(2), 154–156, 158 passim; quiz 162.
- Tallarico, M., Better, H., De Riu, G., & Meloni, S. M. (2016). A novel implant system dedicate to hydraulic Schneiderian membrane elevation and simultaneously bone graft augmentation: An up-to 45 months retrospective clinical study. *Journal of Cranio-Maxillo-Facial Surgery*, 44(8), 1089–1094. <https://doi.org/10.1016/j.jcms.2016.05.016>
- Tatum, H. Jr (1986). Maxillary and sinus implant reconstructions. *Dental Clinics of North America*, 30(2), 207–229.
- Thoma, D. S., Cha, J. K., & Jung, U. W. (2017). Treatment concepts for the posterior maxilla and mandible: Short implants versus long implants in augmented bone. *Journal of Periodontal & Implant Science*, 47(1), 2–12. <https://doi.org/10.5051/jpis.2017.47.1.2>
- Trombelli, L., Minenna, P., Franceschetti, G., Minenna, L., Itró, A., & Farina, R. (2010). Minimally invasive technique for transcresal sinus floor elevation: A case report. *Quintessence International*, 41(5), 363–369.
- Wang, Z. H., Zhang, M. M., Wang, J., Jiang, L., & Liang, Y. H. (2017). Outcomes of Endodontic Microsurgery Using a Microscope and Mineral Trioxide Aggregate: A Prospective Cohort Study. *Journal of Endodontics*, 43(5), 694–698. <https://doi.org/10.1016/j.joen.2016.12.015>
- Wen, S. C., Lin, Y. H., Yang, Y. C., & Wang, H. L. (2015). The influence of sinus membrane thickness upon membrane perforation during transcresal sinus lift procedure. *Clinical Oral Implants Research*, 26(10), 1158–1164. <https://doi.org/10.1111/clr.12429>
- Yassin Alsabbagh, A., Alsabbagh, M. M., Darjazini Nahas, B., & Rajih, S. (2017). Comparison of three different methods of internal sinus lifting for elevation heights of 7 mm: An ex vivo study. *International Journal of Implant Dentistry*, 3(1), 40. <https://doi.org/10.1186/s40729-017-0103-5>

SUPPORTING INFORMATION

Additional supporting information may be found online in the Supporting Information section at the end of the article.

How to cite this article: Gargallo-Albiol J, Sinjab KH, Barootchi S, Chan H-L, Wang H-L. Microscope and micro-camera assessment of Schneiderian membrane perforation via transcresal sinus floor elevation: A randomized ex vivo study. *Clin Oral Impl Res*. 2019;30:682–690. <https://doi.org/10.1111/clr.13453>